Two Critical Cysteine Residues Implicated in Disulfide Bond Formation and Proper Folding of Kir2.1

Hee Cheol Cho,[†] Robert G. Tsushima,[†] The-Tin T. Nguyen,[†] H. Robert Guy,[‡] and Peter H. Backx*[,†]

Departments of Physiology and Medicine, University of Toronto and University Health Network, Toronto, Ontario M5G 2C4, and Laboratory of Mathematical Biology, DCBDC, National Cancer Institute, National Institutes of Health, Bethesda, Maryland 20892

Received October 25, 1999; Revised Manuscript Received January 5, 2000

ABSTRACT: Inwardly rectifying potassium channels are important in cellular repolarization of many excitable tissues. Amino acid sequence alignment of different mammalian inward rectifier K^+ channels revealed two absolutely conserved cysteine residues in the putative extracellular face, suggesting a possible disulfide bond. Replacement of these cysteine residues in the Kir2.1 channel (i.e., C122 and C154) with either alanine or serine abolished current in *Xenopus laevis* oocytes although Western blotting established that the channels were fully expressed. The digestion pattern of channels treated with V8 protease combined with Western blotting under reducing and nonreducing conditions confirmed intrasubunit cross-linking of C122 and C154. Whole-cell and single channel current recordings of oocytes expressing tandem tetrameric constructs with one or two of the mutant subunits suggested that insertion of one mutant subunit is sufficient to eliminate channel function. Coexpression studies confirmed that the cysteine mutant channels eliminate wild-type Kir2.1 currents in a dominant-negative manner. Despite these results, sulfhydryl reduction did not alter the functional properties of Kir2.1 currents. Molecular modeling of Kir2.1 with the two cysteines cross-linked predicted that the extracellular loop between the first transmembrane domain and the pore helix contains a β-hairpin structure. Distinct from the KcsA structure, the disulfide bond together with the β-hairpin structure is expected to constrain and stabilize the P-loop and selectivity filter. Taken together, these results suggest that intramolecular disulfide bond exists between C122 and C154 of Kir2.1 channel and this cross-link might be required for proper channel folding.

Inwardly rectifying K^+ channels play a critical role in membrane excitability of many tissues. Currently, there are at least seven subfamilies of the inward rectifier (Kir1.*x* to Kir7.*x*) (*1*−*3*). These K^+ channels differ from the voltage-gated K^+ channels in primary sequence and contain a common structural motif of two transmembrane segments (M1 and M2) flanking a pore forming (P) region (*1*). Nevertheless, like voltage-gated K^+ channels, four separate Kir gene products coassemble to form a functional channel (*2*, *4*). Previous studies in inward rectifier and voltage-gated K^+ channels have identified pairs of amino acid residues required for pore (P) structure and function (*5*−*7*). Amino acid sequence alignment of Kir2.1[1] (IRK1) with other K^+ channel families revealed the existence of two absolutely conserved cysteine residues (C122 and C154) in mammalian Kir channels that are not found in voltage-gated K^+ channels (Figure 1A). Hydropathy plots of Kir2.1 channels (*8*) predict that C122 and C154 are located on the extracellular face of these channels at the M1-P and P-M2 junctions, respectively. Moreover, recently published crystal structure of KcsA K^+ channel from *Streptomyces lividans*, which has two transmembrane domains flanking a pore-forming unit similar to Kir2.1 (*9*), positioned the M1-P linker and P-M2 linker immediately adjacent to one another (*10*). Taken together, these observations suggest that the conserved C122 and C154 residues in Kir2.1 channel may be linked by a disulfide bond and thereby stabilize pore structure.

In this study, we investigated whether a disulfide bond is formed between C122 and C154 and the possible role of this disulfide bond for channel structure and function. Using a combination of electrophysiological and biochemical methods, we find that C122 and C154 residues form intramolecular disulfide-link and that disruption of this link abolishes the formation of functional channels.

EXPERIMENTAL PROCEDURES

Site-Directed Mutagenesis and Subcloning. Site-directed mutagenesis was performed using uracil-enriched single-stranded DNA according to the methods by Kunkel (*11*). Mutations were confirmed by dideoxy nucleotide sequencing (*12*) (Sequenase kit v2.0, United States Biochemical). In experiments designed to test the functional consequence of mutant C122 and C154 residues, we created tandem tetrameric cDNA constructs similar to that described previously (*13*) and as illustrated in Figure 1B. All constructs were subcloned into the expression vector pGEMHE which contains the 5′ and 3′ UTRs of *Xenopus laevis* oocyte β-globin gene (*14*) and in vitro transcribed using T7 RNA

* To whom correspondence should be addressed. Phone: (416) 340−3272. Fax: (416) 340-4596. E-mail: p.backx@utoronto.ca.
[†] Departments of Physiology and Medicine.
[‡] Laboratory of Mathematical Biology.

[1] Abbreviations: Kir2.1, first member of inward rectifier potassium channel subfamily 2; KcsA, bacterial K^+ channel from *Streptomyces lividans*; WT, wild-type; NG, a double mutant at positions D172N and E224G; DTT, dithiothreitol; UTR, untranslated region; SDS−PAGE, sodium dodecyl sulfate-polyacrylamide gel electrophoresis.

10.1021/bi992469g CCC: $19.00
Published on Web 03/31/2000

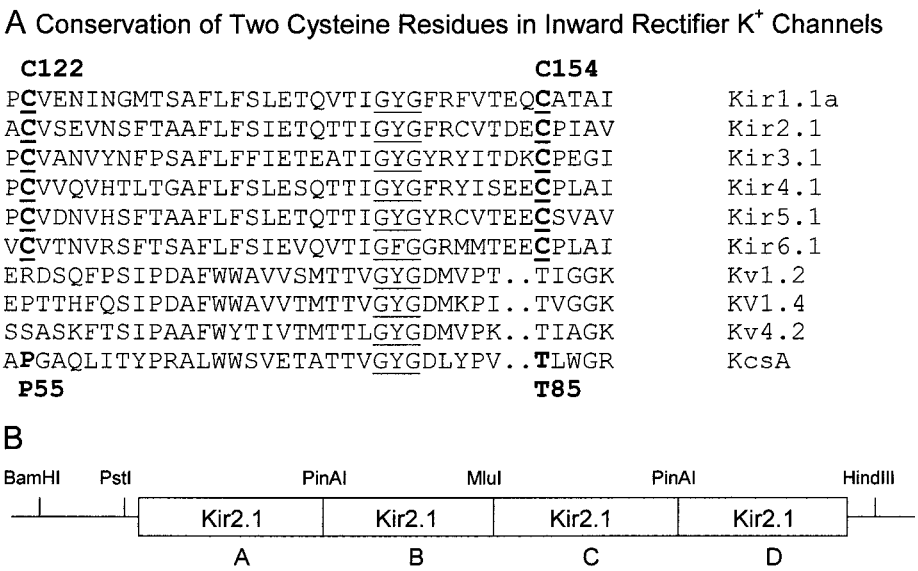

FIGURE 1: Amino acid sequence alignment of different K^+ channels and a schematic drawing of a tandem tetrameric construct for Kir2.1. (A) Amino acid sequence alignment of selected inward rectifier K^+ channels and voltage-gated K^+ channels. The K^+ channel signature sequence (G-Y/F-G) is underlined. C122 and C154 correspond to the residue numbers of Kir2.1 whereas P55 and T85 correspond to the residue numbers of KcsA K^+ channel. (B) A schematic diagram of a tandem tetrameric construct with unique restriction sites used for subcloning.

polymerase (MBI Fermentas). The concentration of the transcribed cRNA was estimated by ethidium bromide staining of 2% agarose gel and spectrophotometry.

Protein Purification and Immunoblotting. Xenopus laevis oocytes were prepared and injected with 1 ng of in vitro transcribed cRNA. After 2 days of injection, individual oocytes were homogenized in ice-cold TBS (20 mM Tris, 150 mM NaCl, 500 μM PMSF, pH 7.4, and 40 μL/oocyte) by repeated suction of oocytes through a 30.5 gauge needle. The homogenized oocytes were spun at 1000*g* for 5 min, and the supernatant was spun again at 120000*g* for 1 h at 4 °C. The pellet was resuspended in 50 mM NH_4HCO_3, pH 7.8, to yield a final protein concentration of 0.85 μg/μL determined using the DC Protein Assay Kit (Bio-Rad). Nonidet P-40 (BDH Laboratory Supplies) (2 μL of 9.3%) in 50 mM NH_4HCO_3 and 3 μL (15 μg) of V8 protease (Sigma) were added to 35 μL of the resuspended membrane preparation (30 μg of protein) (0.5% NP-40 final, pH 7.8) and incubated for 18 h at 37 °C. The reaction mixture was then divided into two equal volumes. To one volume, 2.5 μL of 1 M DTT (100 mM final) and 2.5 μL of 500 mM iodoacetamide (50 mM final) were added and incubated at 60 °C for 20 min (reduced condition). In the second volume, 2.5 μL of 500 mM iodoacetamide (50 mM final) and 2.5 μL of 50 mM NH_4HCO_3 were added and incubated at 60 °C for 20 min (nonreduced condition). The two samples were loaded and run on a 17% SDS−PAGE gel. For undigested Kir2.1 proteins, 15 μg of membrane protein were loaded without the V8 protease treatment.

Western blot was performed using the chemiluminescence system (Amersham). Blocking was carried out in 10% BSA in TBS for 1 h. The Kir2.1 N2 antibody raised in rabbits to a peptide corresponding to amino acids 25−43 of Kir2.1 was used and detected with secondary antibodies to rabbit IgG (raised in donkey) linked to horseradish peroxidase (Amersham). Blots were exposed to film for 15−30 s unless otherwise indicated.

Electrophysiology. Xenopus laevis oocytes were surgically removed from the anesthetized frogs, washed in Ca-free OR-2 solution (in millimolar, 88 NaCl, 2 KCl, 1 $MgCl_2$ and 5 mM Hepes, pH 7.6), and treated with 1.5 mg/mL collagenase for 1 h. The separated oocytes were washed with ND96 solution (in millimolar, 96 NaCl, 1 $BaCl_2$, 1 $MgCl_2$, and 5 mM Hepes, pH 7.6). Oocytes were injected with 50 nL of cRNA of known concentration determined by spectrophotometry and ethidium bromide staining on a 2% agarose gel. Whole-cell currents were recorded 1−3 days after injection using a two-electrode voltage-clamp amplifier (OC-725A; Warner Instruments) at room temperature (21−23 °C). Agarose-plugged microelectrodes (TW120F-6; World Precision Instrument) were filled with 3 M KCl and had a final resistance of 1−3 MΩ for voltage-sensing electrode and 0.5−1 MΩ for current-recording electrode. The extracellular solution ("High K^+" solution) contained 90 mM KCl, 3 mM $MgCl_2$, 0.3 mM niflumic acid, and 10 mM Hepes, pH adjusted to 7.4 with KOH. Currents were elicited by a 300 ms test pulse from −100 to +100 mV in 10 mV increments from a holding potential of 0 mV or by voltage ramps from −100 to +100 mV applied for 350 ms. All current recordings are presented as Ba^{2+}-subtracted currents in order to eliminate leak. For testing the redox sensitivity of WT Kir2.1 channels, DTT (Calbiochem) and bis-2-mercaptoethyl sulfone (BMS, Calbiochem) were used.

Single channel recordings were performed using the Axopatch 200A amplifier (Axon Instruments). Vitelline membranes were mechanically removed from oocytes incubated in a hyperosmotic solution (in millimolar, 280 potassium-glutamate, 20 KCl, 10 Hepes, and 1 $MgCl_2$, pH 7.4). During recording, the oocyte was bathed in a solution containing 110 mM KCl, 10 mM Hepes, 9 mM EGTA, 1 mM EDTA, and 200 μM $CaCl_2$ (pH adjusted to 7.3 with KOH). Recording glass pipets (TW150F-4, WPI) were filled with a solution of 130 mM KCl, 10 mM Hepes, and 3 mM $MgCl_2$ (pH adjusted to 7.3 with KOH; total $[K^+]$ =

~140 mM) and had resistances of 6−10 MΩ. Current records were filtered at 1 kHz with a Bessel filter.

Statistics. To assess the ability of mutant monomeric proteins to eliminate wild-type Kir2.1 currents in a dominant-negative manner, we compared the measured currents produced in oocytes following injection of various ratios of WT and mutant monomers with the predicted current using the binomial distribution function (see Results)

$$g(y) = [4!/\{y!(4-y)!\}]p^y(1-p)^{n-y}$$

where y is the number of wild-type subunits incorporated into a channel, $y = 0$, 1, 2, 3, and 4 and p is the probability of the wild-type subunit being incorporated into a channel (assumed to be proportional to the relative quantity of wild-type Kir2.1 cRNA injected into the oocyte). For this analysis, we assume that four wild-type monomers must be present to produce a functional channel. For instance, when equivalent amounts of wild-type and mutant cRNA are injected, the probability of producing functional channels is 6%.

Data presented are the means ± SE. Statistical significance was determined using an unpaired Student's *t*-test with $P < 0.05$ representing significance.

RESULTS

Replacement of C122 and C154 Residues Disrupts a Disulfide Bond and Channel Function. To examine the functional role of C122 or C154 in Kir2.1 channels, these residues were replaced with serine or alanine. As shown in Figure 2A, oocytes injected with mutant Kir2.1 channels, C122S and C154S, did not yield measurable Ba^{2+}-sensitive currents in contrast to oocytes injected with wild-type Kir2.1 (WT) channels. Similarly, no detectable current was observed in oocytes injected with the corresponding alanine mutant (i.e., C122A and C154A) or the double mutant (i.e., C122S/C154S or C122A/C154A) channels (data not shown). Despite the absence of current, the amount of channel protein expressed was similar between C122S, C154S, and WT channels as shown in Figure 2B.

On the basis of the absence of current in C122S, C154S, and C122S/C154S channels, we hypothesized that C122 and C154 might form a disulfide link. This hypothesis is supported by the absolute conservation of C122 and C154 in mammalian Kir channels combined with the putative locations of these residues in the nonreducing extracellular face of Kir channels (*8*). To test this hypothesis, we examined the protein mobility of WT and mutant channels on an 8.5% SDS−PAGE gel under reducing and nonreducing conditions. Using immunoblots of crude membrane extracts from oocytes run on denaturing polyacrylamide gels, Figure 2B shows that the molecular weight of WT channels under reducing conditions (i.e., in the presence of 100 mM DTT) was estimated to be about 51 kDa compared with the predicted molecular mass of 49 kDa (i.e., 428 amino acids). Figure 2B further establishes that WT channels migrated faster under nonreducing (−) than reducing conditions (+), with the mobility of WT channels in reducing condition being indistinguishable from that of mutant channels under either nonreducing or reducing conditions. These results are consistent with the existence of a disulfide bond between C122 and C154 in a single subunit and suggest that the

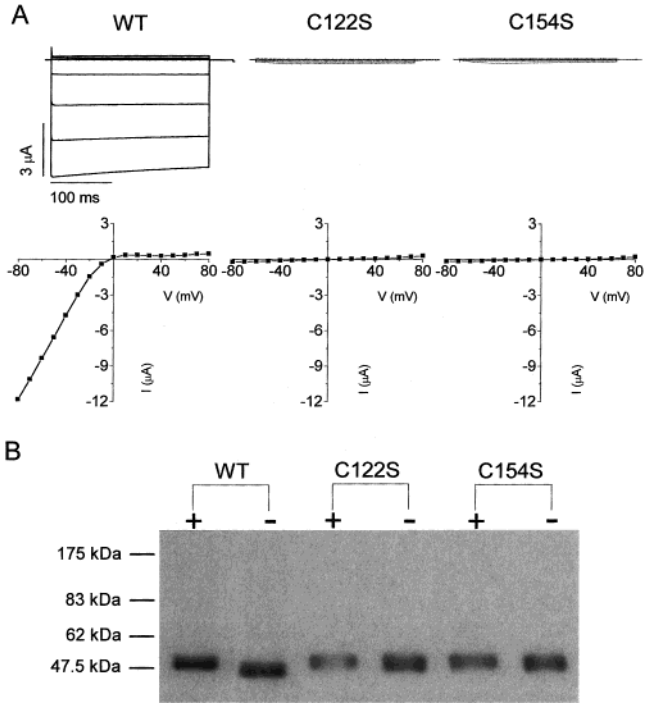

FIGURE 2: C122S and C154S mutations in Kir2.1 result in the knockout of the channel function. (A) (Top) Representative whole cell current traces from oocytes injected with WT, C122S, or C154S monomeric cRNA. Currents were elicited by a 300 ms test potential of −100 to +100 mV in 10 mV increments from a holding potential of 0 mV. Every other traces are shown here. (Bottom) Current−voltage (I−V) relations in whole cell recording are shown for the respective sample traces above. The steady-state current was measured at the end of the 300 ms test pulse. (B) Western blot of denaturing polyacrylamide gel showing different Kir2.1 monomers. A total of 0.5 ng of monomeric cRNAs encoding WT, C122S, and C154S were injected into *Xenopus* oocytes. The oocytes injected with 1 ng of WT cRNA gave rise to greater than −20 μA current at −80 mV at 24 h after injection. For each lane, 5 μg of total oocyte membrane protein were loaded and run on an 8% SDS−PAGE gel under reducing [(+) 100 mM DTT) and nonreducing [(−) no DTT] conditions, followed by immunoblot with the N-terminal Kir2.1 antibody.

disulfide bond is disrupted by either 100 mM DTT or a point mutation (i.e., C122S or C154S) leading to a mobility shift.

The presence of an intramolecular disulfide bond between C122 and C154 was further verified by partial selective proteolysis using V8 protease, an enzyme that selectively cleaves at glutamate residues in the presence of, pH 7.8, NH_4-HCO_3 buffer (*15*, *16*). To assist in their interpretation, these studies were performed on Kir2.1 channels in which the residue E63 was replaced with an aspartate residue (E63D). E63D mutant channels produced oocyte currents indistinguishable from WT channels (data not shown). If a disulfide link exists between C122 and C154, then the shortest amino-terminal fragment expected in these E63D channels following V8 protease treatment has a predicted molecular mass of approximately 19 kDa (corresponding to digestion at E191) in nonreducing conditions and only about 17 kDa (corresponding to digestion at E125) after reduction with DTT. Consistent with our expectations, reduction after V8 protease treatment of E63D channel proteins yielded a minor digestion fragment (band "B") having an apparent molecular mass of 18 kDa (Figure 3B, lane 2) which was absent in nonreducing conditions (Figure 3B, lane 1). When the WT channel proteins were incubated with V8 protease in the continued

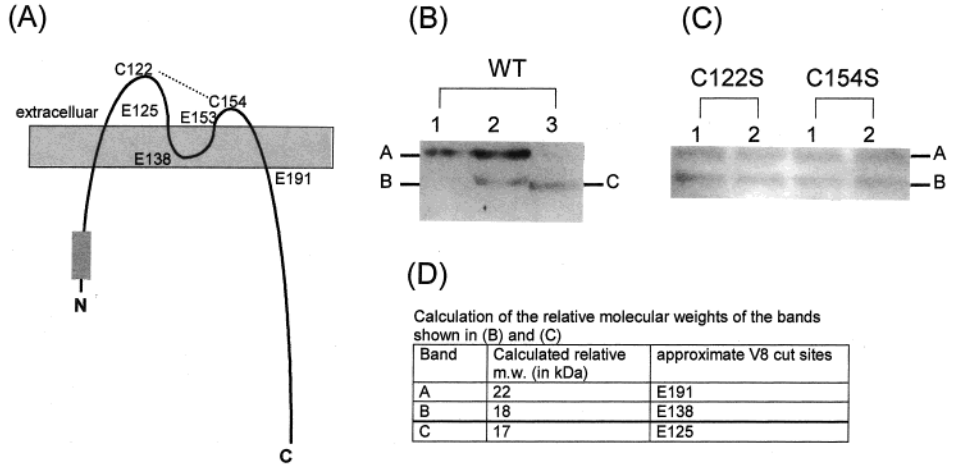

FIGURE 3: C122 and C154 form an intramolecular disulfide bond. (A) A schematic diagram showing approximate locations of the Kir2.1 glutamate residues proximal to the N-terminus. The N-terminal Kir2.1 antibody recognizes the amino acids 25−43 as indicated with a rectangle. (B, C) Western blot showing the result of V8 protease digestion of monomeric WT Kir2.1 protein (B) and C122S and C154S monomers (C) in the absence (lane 1) and presence (lane 2) of 100 mM DTT. For panel B, reactions were carried out either in the absence (lanes 1 and 2) or in the presence of 20 mM DTT (lane 3) for 40 h at 37 °C. At the end of the digestion, the reaction was divided into two equal amounts and treated with (lane 2) or without (lane 1) 100 mM DTT. For (C) the reactions were carried out for 18 h at 37 °C without any DTT. All the constructs were made in E63D background. The digested reaction was run on a 17% SDS−PAGE gel followed by the immunoblot and chemiluminescence. (D) Calculated relative molecular weights of bands in panels B and C and the approximate V8 protease cleavage sites.

presence of 20 mM DTT, there was only one major band (Figure 3B, lane 3, band C), suggesting a complete proteolysis. Interestingly, the mobility of band C was somewhat faster than that of band B in Figure 3B. This observation can be explained if E138 is the preferred V8 recognition site when digestion reactions are carried under nonreducing conditions whereas E125 is preferred under reducing conditions (Figure 3D). The V8 digestion pattern of C122S and C154S channels were unaffected by the redox state and were identical to the digestion pattern of the WT channels under reducing conditions (Figure 3, panels B and C). These results further establish that C122 and C154 residues are cross-linked by intramolecular disulfide bond.

C122S, C154S, and C122S/C154S Mutants Do Not Participate in Functional Channel Formation. The results in Figures 2 and 3 show that removal of the disulfide cross-link between C122 and C154 by mutagenesis disrupts channel function but not protein expression. It is conceivable that the absence of current observed in oocytes injected with these mutant channels resulted from the presence of four mutations in the tetrameric channels. In other words, the channels might be functional if the tetrameric proteins contained less than four mutations. To explore the nature of the disruption of channel function further, tandem tetrameric DNA constructs were created by linking four channel subunits together in a single open reading frame (*13*, *14*) (Figure 1B). For equivalent amounts of injected cRNA, expression of tandem constructs containing a single mutation in position A [i.e., C122S-$(WT)_3$ or C154S-$(WT)_3$] yielded average currents that were about 25-fold lower [i.e., -1.2 μA $\pm$ 0.6, $n = 10$, for C122S-$(WT)_3$ and -0.9 ± 0.6 μA, $n = 10$, for C154S-$(WT)_3$ channels] than $(WT)_4$ channels (-24.2 ± 1.7 μA, $n = 10$) measured at -80 mV. Despite marked reductions in current amplitude, the macroscopic I−V relationships of the currents produced by these two mutant channels were indistinguishable from that of $(WT)_4$ channels. Similar results were observed in WT-C122S-$(WT)_2$ and WT-C154S-$(WT)_2$ channels where a mutant subunit is introduced at the second subunit from the N-terminus (data not shown). In contrast, introduction of two or more mutant subunits in these tetrameric channels yielded no measurable current regardless of the position or type of mutation [i.e., X-WT-X-WT, $(X)_2$-$(WT)_2$, or $(X)_3$-WT, where X = C122S or C154S], even 3 days following cRNA injection.

The observation that C122S-$(WT)_3$ and C154S-$(WT)_3$ channels produced finite currents while two or more mutations in one tandem tetrameric channel produced no detectable current could arise for two reasons. First, one mutation might be tolerated while a second is sufficient to eliminate channel function completely. Alternatively, a functional channel might be formed by coassembly of two X-$(WT)_3$ channel proteins as previously demonstrated for tandem trimeric Kir2.1 proteins (*4*), and tandem tetrameric voltage-gated K^+ channels (*14*, *17*). To distinguish between these two possibilities, we created tandem tetrameric cDNA constructs in which each subunit contained the mutations D172N and E224G (NG) that have been previously shown to markedly reduce the rectification properties of Kir2.1 currents (*4*). Figure 4A shows representative I−V relationships recorded in oocytes injected with $(WT)_4$ compared to $(NG)_4$ (left panels). As expected the outward current magnitude produced by $(NG)_4$ channels at voltages above E_K were much larger than $(WT)_4$ channels. Figure 4A also demonstrates that incorporation of one wild-type subunit in the NG background [i.e., WT-$(NG)_3$] is sufficient to confer WT rectification properties to the measured current, consistent with a previous report (*4*). For quantification purposes, the degree of rectification was assessed by calculating the ratio of current recorded at +40 mV to that recorded at −40 mV (i.e., I_{+40}/I_{-40}) (*4*), and the results of such analysis are summarized in Figure 4B. The ratio I_{+40}/I_{-40} was 0.031 ± 0.004 ($n = 10$) for $(WT)_4$ which was indistinguishable ($P > 0.05$) from 0.034 ± 0.003 ($n = 12$) recorded in WT-$(NG)_3$ injected oocytes but very different ($P < 0.05$) from 0.47 ± 0.06 ($n = 12$) measured for $(NG)_4$ channels.

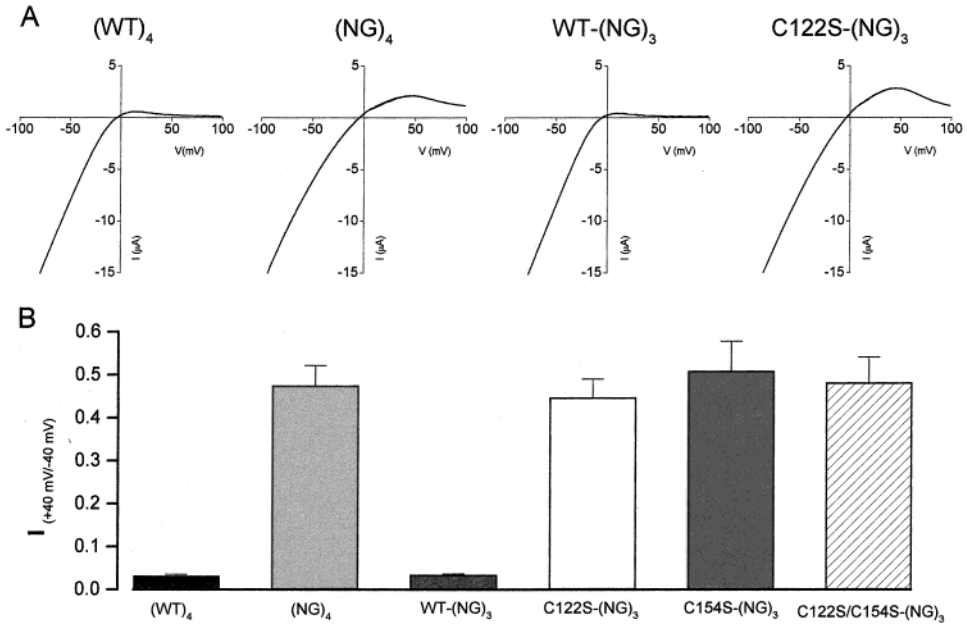

FIGURE 4: Mutant subunits containing C122S, C154S, or C122S/C154S do not participate in forming a functional channel in tandem tetrameric channels. (A) Representative whole cell currents from oocytes injected with 0.5 ng of WT, $(NG)_4$ and WT-$(NG)_3$ constructs and recorded 24 h later. For C122S-$(NG)_3$, 2 ng of cRNA was injected and whole cell currents were recorded in 72 h when comparable currents could be measured. Currents were generated by voltage ramps from −100 to +100 mV applied for 350 ms. (B) Bar graph showing the ratios of outward current at +40 mV to inward current at −40 mV from different tandem tetrameric constructs.

Next, we created X-$(NG)_3$ tandem constructs in which "X" represents subunits containing C122S, C154S, or C122S/C154S mutations in a WT background with respect to channel rectification (i.e., "X" subunits retain D172 and E224 residues). As summarized in Figure 4B, I_{+40}/I_{-40} for C122S-$(NG)_3$, C154S-$(NG)_3$, and C122S/C154S-$(NG)_3$ channels were indistinguishable from $(NG)_4$ channels. [i.e., 0.45 ± 0.04 ($n = 8$), 0.51 ± 0.07 ($n = 8$), and 0.48 ± 0.06 ($n = 8$), respectively] while the magnitude of the X-$(NG)_3$ currents were considerably reduced compared to WT-$(NG)_3$ or $(NG)_4$. When 1 ng of each of the tetrameric cRNA was injected into oocytes, the current amplitudes measured after 24 h at −80 mV were −32.4 ± 1.7 and −16 ± 1.5 μA for WT-$(NG)_3$ and $(NG)_4$, respectively, while C122S-$(NG)_3$, C154S-$(NG)_3$, and C122S/C154S-$(NG)_3$ produced −0.9 ± 0.4, −0.7 ± 0.4, and −1.0 ± 0.3 μA, respectively ($n = 8$ for each construct). Complementary results were obtained when C122S or C154S monomers with wild-type rectification properties were coexpressed with NG monomers; the resultant currents were indistinguishable from the current exhibited by the expression of NG monomer alone (data not shown). For oocytes expressing C122S:NG (1:3 ratio), C154S:NG (1:3 ratio), or NG alone, the calculated I_{+40}/I_{-40} values were 0.34 ± 0.05 ($n = 8$), 0.31 ± 0.05 ($n = 8$), and 0.35 ± 0.04 ($n = 10$), respectively ($P > 0.05$). From these studies we concluded that a functional channel is formed by coassembly of two X-$(WT)_3$ channel proteins.

The results above suggest that incorporation of a single monomer with the C122S or C154S mutation is sufficient to eliminate channel function. This conclusion is consistent with single channel recordings of the different tandem tetrameric channels. If one cysteine mutant is tolerated, the decreased whole-cell current amplitudes in X-$(WT)_3$ channels compared to $(WT)_4$ channels might arise from decreased single channel conductance or decreased mean open time or both. As summarized in Figure 5A, $(WT)_4$, C122S-$(WT)_3$, and C154S-$(WT)_3$ channels had the typical long open time characteristic of WT Kir2.1 channel and yielded identical single channel conductance values of 21.1 ± 0.6 pS ($n = 2$), 22.4 ± 0.9 pS ($n = 3$), and 21.0 ± 0.7 pS ($n = 3$), respectively (Figure 5B). This is nearly identical to the single channel conductance of 21.4 pS published previously for Kir2.1 channels (*8*).

C122S and C154S Mutants Behave in a Dominant-Negative Fashion. Figure 6A shows that coinjecting 0.2 ng of WT cRNA and the equal amount of C122S cRNA produced an average current of −0.4 ± 0.3 μA ($n = 7$, Δ) measured at −80 mV. This current was significantly less ($P < 0.05$) than the current observed when 0.2 ng of WT cRNA were injected alone [−4.4 ± 0.7 μA, $n = 7$ (□)]. Similarly, reduced current magnitudes were observed when C154S or C122S/C154S monomers were coexpressed with the WT monomer [Figure 6A (▽ and ◇)]. The amount of cRNA used for these coinjections did not result in saturation of the oocyte expression systems since a 2-fold increase in WT cRNA to 0.4 ng increased the measured current at −80 mV to −9.2 ± 0.5 μA [$n = 7$ (○)].

If C122S or C154S mutants truly behave in a dominant-negative manner, then channels will be functional only when all four subunits are WT. Figure 6B summarizes the results of the relative measured current recorded in oocytes injected with various ratios of WT to mutant channels [i.e., (○) C122S and (△) C154S]. The predicted probability for forming a (functional) channel containing four WT proteins, using the binomial distribution function, is illustrated by the solid line in Figure 6B and shown to correspond remarkably well with the measured relative currents. Similar results were found when different amounts of NG monomeric cRNA were coinjected with either C122S or C154S monomeric cRNA (data not shown). These results establish that C122S and C154S mutant channels act in a dominant-negative manner to eliminate WT channel function.

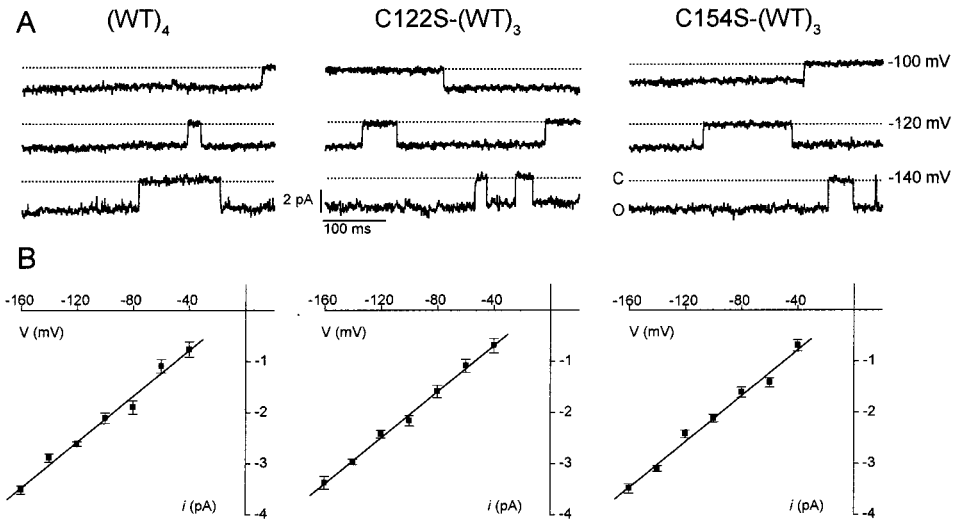

FIGURE 5: Single channel activities of the mutant tetramers show the similar behavior as the $(WT)_4$ channels. (A) Representative single-channel records elicited by voltage steps to various potentials from a holding potential of 0 mV in the cell-attached patch mode for $(WT)_4$ (left panel), C122S-$(WT)_3$ (middle panel), and C154S-$(WT)_3$ (right panel). The dashed lines indicate the zero current level. (B) I−V plot of the single channel current in panel A. Linear regression lines were fitted to the plots. Average single channel conductances were calculated by averaging the conductance values from each patch, yielding (from left to right) 21.1 ± 0.6 pS (n = 2), 22.4 ± 0.9 pS (n = 3), and 21.0 ± 0.7 pS (n = 3).

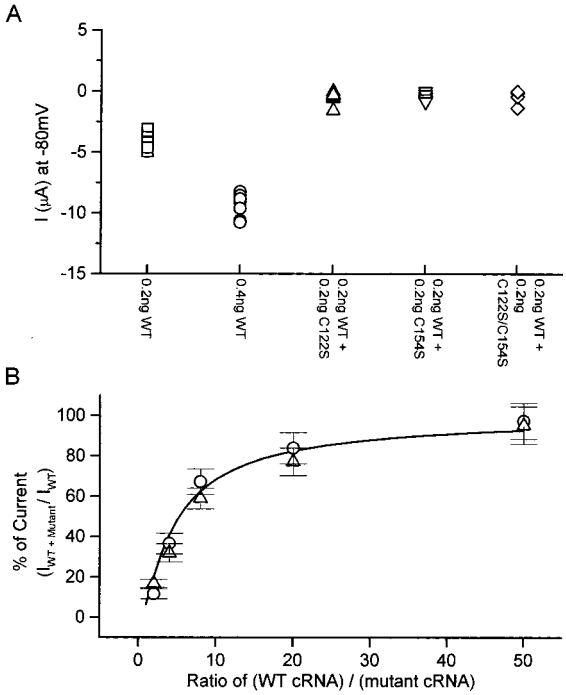

FIGURE 6: Monomeric C122S and C154S mutants show dominant negative behavior. (A) Wild-type monomeric cRNA was injected alone or with the equal amount of monomeric mutant cRNA. Current was measured 24 h after the injection. The steady-state current was measured at the end of 300 ms test potential at −80 mV. (B) Five different ratios of WT:C122S (○) or WT:C154S (△) cRNA were injected into oocytes (2:1, 4:1, 8:1, 20:1, and 50:1). The steady-state current was measured at the end of 300 ms test potential at −80 mV. The currents were normalized with the oocytes injected with 0.5 ng of the WT cRNA, which produced 23.3 ± 0.9 μA current 24 h after the injection. The predicted pattern of current expression by binomial distribution function when one mutant subunit is sufficient to knockout the channel function is represented by the solid line.

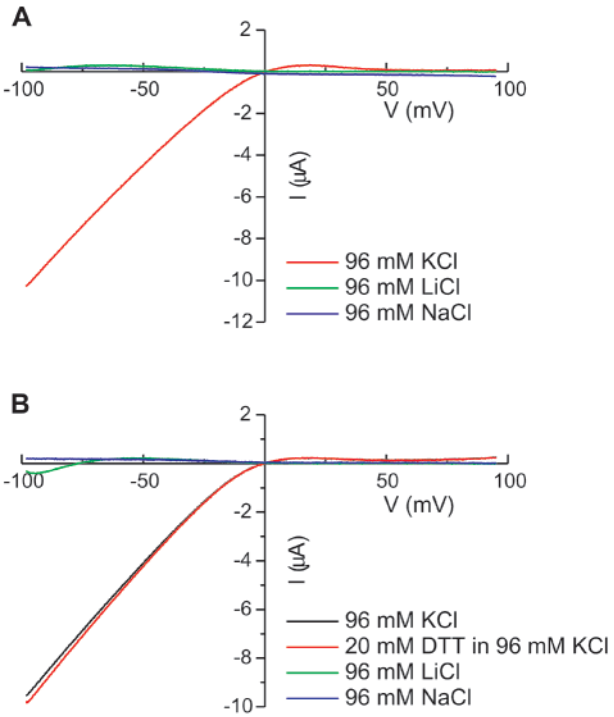

FIGURE 7: Selectivity of WT monomer is unaffected after channel reduction with 20 mM DTT. (A) Representative whole cell currents from an oocyte injected with 0.2 ng of WT Kir2.1 monomeric cRNA and recorded 24 h later. Currents were generated by voltage ramps from −100 to +100 mV applied for 350 ms. The traces were collected as different solutions were being washed beginning with the control solution (96 mM KCl), 96 mM LiCl, and then 96 mM NaCl. (B) Before replacing the control bath with Li^+- or Na^+-containing bath, 30 mL of 20 mM DTT was washed in to reduce any disulfide bond.

Kir2.1 Channel Currents Are Insensitive to the Redox State. One might predict that if cross-linking between C122 and C154 were critical for channel function, then the properties of currents produced by Kir2.1 channels might be sensitive to the redox state. However, extracellular application of 20 mM DTT for periods in excess of 15 min did not affect either current amplitudes or permeability to Li^+ or Na^+ (Figure 7). Application of the more powerful reducing agent *bis*-2-mercaptoethyl sulfone (BMS) (*18*) reduced the slope conductance of Kir2.1 currents by 50%

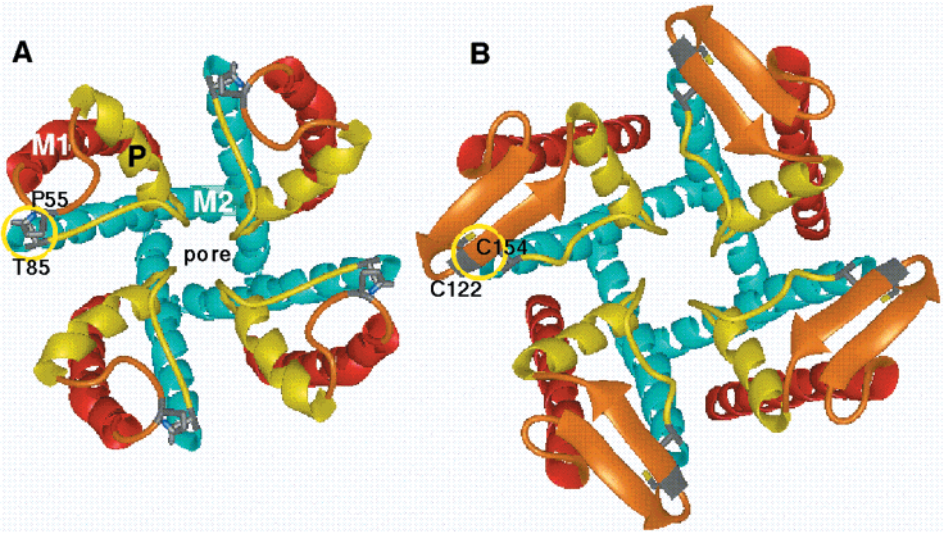

FIGURE 8: Molecular models of Kir2.1 and KcsA K^+ channel pore regions. Ribbon representations of the KcsA structure and molecular models of the Kir2.1 channel. Helices and β-strands are represented by ribbons and coiled segments by thin tubes. The view is from outside the cell down the axis of the pore. (A) Representation of the crystal structure of KcsA. The residues, P55 and T85, that align with C122 and C154 of Kir2.1 are colored by atom and circled in yellow. (B) Molecular model of the Kir2.1 channel modeled after the KcsA structure with adjustments to increase hydrogen bonding of polar groups and to form a disulfide bridge between C122 and C155 (circled in yellow).

but this effect of BMS was rapidly reversed during washout, suggesting a direct blocking action of this agent (data not shown). Thus, despite cross-linking of C122 and C154 and the role of cross-linking in forming functional channels, changes in redox state do not result in measurable electrophysiological alterations of fully assembled Kir2.1 channels.

DISCUSSION

The mobility shifts observed in Western Blots with WT, C122S, C154S, and C122S/C152S channel proteins under reducing and nonreducing conditions as well as the absence of high molecular weight adducts corresponding to dimers, trimers, and tetramers are consistent with an intramolecular disulfide bond between C122 and C154 in Kir2.1 channels. The V8 digestion pattern confirmed the presence of a disulfide link; under nonreducing conditions, V8 digestion only yielded one major fragment corresponding roughly to cleavage at E191, despite the existence of three potential cleavage sites between C122 and C154 (Figure 3B, lane 1). Treatment of the digested samples with DTT resulted in the appearance of one additional band (Figure 3B, lane 2) corresponding roughly to digestion at residue E138. Interestingly, the bands corresponding to digestion at positions E125 and E153 appeared to be absent, suggesting that not all the sites are equally susceptible to V8 digestion under nonreducing conditions. Preferential digestion of selected sites by V8 has been reported previously for other proteins (*19*, *20*). By contrast, V8 digestion of WT under reducing conditions and V8 digestion of mutant channels (i.e., C122S or C154S) under reducing or nonreducing conditions yielded a single band with mobility expected for digestion at E125. Taken together, these results establish the presence of a disulfide bond between C122 and C154 that interferes with V8 digestion at positions E125 and E153, possibly because these residues are buried.

Mutation of C122 and C154 alone, or together, reduced current in a dominant-negative fashion establishing that incorporation of a single mutant subunit is sufficient to disrupt channel function. Dominant-negative inhibition of current by these mutant channels was further supported by the single channel measurements showing that the unitary currents were identical between $(WT)_4$, C122S-$(WT)_3$, and C154S-$(WT)_3$ channels (Figure 5). However, the presence of measurable currents in oocytes following injection of C122S-$(WT)_3$ and C154S-$(WT)_3$ channels would only be possible if functional channels were created by coassembly of two or more separate tandem proteins. This conjecture was confirmed in our expression studies of tandem tetrameric constructs in which C122 or C154 subunit retained the strong rectification properties of WT Kir2.1 while the subunits lacking these mutations had the NG (D172N/E224G) mutations which disrupt strong rectification. In these experiments, the currents displayed rectification properties expected only if all four subunits carried the NG mutation which can only occur if channels were coassembled from two separate tandem genes (*4*). These studies further demonstrate that coassembly of distinct tandem-tetrameric channels does not occur in a random fashion since the current amplitudes were 2-fold larger in C122S-$(NG)_3$ and C154S-$(NG)_3$ than in NG-C122S-$(NG)_2$ and NG-C154S-$(NG)_2$ channels (data not shown). These data suggest that channel formation most commonly involves the contribution of three subunits from one tetramer with a single subunit from another tandem tetramer.

Our observation that one subunit lacking the NG mutation [i.e., WT-$(NG)_3$] is sufficient to restore normal rectification as seen in $(WT)_4$ channels is consistent with a previous report (*4*). Using inside-out macropatches, Yang et al. found that the affinity of WT-$(NG)_3$ channels for spermidine block was about 16% of $(WT)_4$ channels (*4*). However, a number of other cellular factors, other than spermidine, can also cause inward rectification in Kir2.1 channels (*21*). Similarly, graded rectification responses with different numbers of WT subunits by spermidine were also demonstrated in a strong inward rectifier BIR10 channels (*22*). Since our results are obtained in whole oocytes that contain undetermined levels of these various blocking agents, it is unclear how differences in spermidine affinities will affect the rectification properties

of WT-$(NG)_3$ channels in comparison to $(WT)_4$ channels. Specifically, other polyamines or Mg^{2+} might be the primary determinants of rectification in Kir2.1-based currents when recorded in whole oocytes, and the effectiveness of these other blocking particles to produce inward rectification might not differ between WT-$(NG)_3$ and $(WT)_4$ channels. Indeed, Yang et al. (*4*) found that Mg^{2+} was equally effective in blocking these two tandem channels. Alternatively, the level of spermidine within the oocyte in our studies might be sufficiently high to cause equal degrees of rectification in WT-$(NG)_3$ and $(WT)_4$.

The inability of reducing agents to affect current properties (Figure 7) combined with the dominant-negative property of C122S and C154S mutant channel proteins suggests that the disulfide link might be critical for proper channel folding but is less crucial after the channels have been assembled. In other words, once the channel achieves its native structure, destruction of the disulfide bond is insufficient to disrupt channel structure either because the disulfide bond can reform rapidly or because the native structure is stabilized by many other interactions, thereby mitigating the need for a disulfide link.

The sequence alignment of inward rectifiers and voltage-gated K^+ channels reveals that the P-loops of all mammalian inward rectifier K^+ channels, but not voltage-gated or KcsA K^+ channels, contain two absolutely conserved pore cysteines at analogous positions to those in the Kir2.1 channels (Figure 1A). This observation suggests that these cysteine residues might also be cross-linked in other mammalian inward rectifier channels besides Kir2.1 thereby underling a common structural architecture in mammalian inward rectifier K^+ channels. In this regard, it is important to note that the conserved cysteines are separated by precisely 32 residues in all mammalian inward rectifier channels. To explore the possible structural implications of a disulfide link between C122 and C154 in Kir2.1 channels, we performed molecular modeling studies using methods described previously (*23*, *24*). In these modeling studies, we assumed that the pore structure of Kir2.1 channels was similar to that reported recently for the crystallized KcsA channel (*10*). While this assumption seems reasonable, recent mutagenesis studies revealed that the packing relationship between M1 and M2 within the subunit appears to differ between Kir2.1 and KcsA channels (*25*). The extent to which these differences apply to the outer pore and P-loop region remains to be determined. Nevertheless, the residues P55 and T85 in KcsA K^+ channel, which are analogous to the cross-linked cysteines in Kir2.1 channels, are immediately adjacent to one another and flank the pore helix as well as selectivity filter of the P-loop. The sequence alignments in Figure 1A demonstrate that Kir2.1 channels, like other mammalian inward rectifier channels, have a relatively long segment that connects the C-terminal end of M1 to the beginning of the P-loop helix when compared to KcsA, as well as voltage-gated K^+ channels. To accommodate these extra residues, we modeled the long M1−P segment of Kir2.1 as a β-hairpin structure (Figure 8B) rather than a random coil as seen in the KcsA channel. Analogous to its role in other proteins (*26*), this β-hairpin structure is energetically stable which, along with the disulfide link, severely constrains the long M1−P segment thereby stabilizing the P-helix and the selectivity filter into a conformation resembling the KcsA structure (*10*). The multiple possible interactions between the β-hairpin and the remainder of the channel protein might also explain our observation that the application of reducing agents had no effect on channel function, further supporting a primary role of the disulfide link in guiding the proper protein folding (*27*, *28*).

Previous studies have demonstrated that electrostatic interactions between residues in the P-loop and M2 regions are important for maintaining pore structure by forming a salt bridge (*5*). On the basis of these studies, we attempted to reconstitute the interactions between C122 and C154 by replacing these residues with aspartate and lysine, respectively, but this did not rescue channel function (data not shown). These results suggest that electrostatic ionic interactions are of insufficient strength or that disulfide links are essential for ensuring proper protein structure, as established for many other proteins requiring chaperon proteins (*29*) and for Cu, Zn superoxide dismutase (*30*).

Our results indicate that a disulfide bond exists between C122 and C154 of Kir2.1 and that this bond appears to be critical for proper channel folding. Molecular modeling studies showed that this disulfide bond constrains the relatively long M1-P linker in the P-loop of Kir2.1 into a stable β-hairpin structure, which is not present in the pore of KcsA K^+ channel. Given the absolute conservation of the two cysteine residues among all mammalian inward rectifiers, the disulfide bond in the pore might be a common feature of the outer pore of these channel, necessary for achieving the proper tertiary channel structure.

ACKNOWLEDGMENT

All correspondence should be addressed to P. H. B. We thank Dr. Lily Y. Jan for providing us with Kir2.1 clone and the N-terminal Kir2.1 antibody and critical reading of the manuscript. This work was supported by Medical Research Council of Canada to P.H.B. Equipment grants from the Alan Tiffin Trust are gratefully acknowledged. P.H.B holds a Career Investigator Award from the Heart and Stroke Foundation of Ontario and a Premier's Excellence Award for Research from the Government of Ontario.

REFERENCES

1. Doupnik, C. A., Davidson, N., and Lester, H. A. (1995) *Curr. Opin. Neurobiol. 5*, 268−277.
2. Nichols, C. G., and Lopatin, A. N. (1997) *Annu. Rev. Physiol. 59*, 171−191.
3. Coetzee, W. A., Amarillo, Y., Chiu, J., Chow, A., Lau, D., McCormack, T., Moreno, H., Nadal, M. S., Ozaita, A., Pountney, D., Saganich, M., Vega-Saenz de Miera, E., and Rudy, B. (1999) *Ann. N.Y. Acad. Sci. 868*, 233−285.
4. Yang, J., Jan, Y. N., and Jan, L. Y. (1995) *Neuron 15*, 1441−1447.
5. Yang, J., Yu, M., Jan, Y. N., and Jan, L. Y. (1997) *Proc. Natl. Acad. Sci. U.S.A. 94*, 1568−1572.
6. Kirsch, G. E., Drewe, J. A., Hartmann, H. A., Taglialatela, M., de Biasi, M., Brown, A. M., and Joho, R. H. (1992) *Neuron 8*, 499−505.
7. Kirsch, G. E., Drewe, J. A., De Biasi, M., Hartmann, H. A., and Brown, A. M. (1993) *J. Biol. Chem. 268*, 13799−804.
8. Kubo, Y., Baldwin, T. J., Jan, Y. N., and Jan, L. Y. (1993) *Nature 362*, 127−133.
9. Schrempf, H., Schmidt, O., Kummerlen, R., Hinnah, S., Muller, D., Betzler, M., Steinkamp, T., and Wagner, R. (1995) *EMBO 14*, 5170−5178.

10. Doyle, D. A., Cabral, J. M., Pfuetzner, R. A., Kuo, A., Gulbis, J. M., Cohen, S. L., Chait, B. T., and MacKinnon, R. (1998) *Science 280*, 69−77.
11. Kunkel, T. A. (1985) *Proc. Natl. Acad. Sci. U.S.A. 82*, 488−492.
12. Sanger, F., Nichlen, S., and Coulson, A. R. (1977) *Proc. Natl. Acad. Sci. U.S.A. 74*, 5463−5467.
13. Yang, J., Jan, Y. N., and Jan, L. Y. (1995) *Neuron 14*, 1047−1054.
14. Liman, E. R., Tytgat, J., and Hess, P. (1992) *Neuron 9*, 861−871.
15. Drapeau, G. R., Boily, Y., and Houmard, J. (1972) *J. Biol. Chem. 247*, 6720−6726.
16. Houmard, J., and Drapeau, G. R. (1972) *Proc. Natl. Acad. Sci. U.S.A. 69*, 3506−3509.
17. McCormack, K., Lin, L., Iverson, L. E., Tanouye, M. A., and Sigworth, F. J. (1992) *Biophys. J. 63*, 1406−1411.
18. Singh, R., Lamoureux, G. V., Lees, W. J., and Whitesides, G. M. (1995) *Methods Enzymol. 251*, 167−173.
19. Trainer, V. L., Brown, G. B., and Catterall, W. A. (1996) *J. Biol. Chem. 271*, 11261−11267.
20. Mitchell, J., and Mayeenuddin, L. H. (1998) *Biochemistry 37*, 9064−9072.
21. Lopatin, A. N., Makhina, E. N., and Nichols, C. G. (1994) *Nature 372*, 366−369.
22. Glowatzki, E., Fakler, G., Brandle, U., Rexhausen, U., Zenner, H. P., Ruppersberg, J. P., and Fakler, B. (1995) *Proc. R. Soc. London, Ser. B 261*, 251−261.
23. Durell, S. R., and Guy, H. R. (1992) *Biophys. J. 62*, 238−247.
24. Durell, S. R., and Guy, H. R. (1999) *Biophys. J. 77*, 789−807.
25. Minor, D. L., Jr., Masseling, S. J., Jan, Y. N., and Jan, L. Y. (1999) *Cell 96*, 879−891.
26. Wang, Y., and Shortle, D. (1995) *Biochemistry 34*, 15895−15905.
27. Matsumura, M., Signor, G., and Matthews, B. W. (1989) *Nature 342*, 291−293.
28. Zhang, T., Bertelsen, E., and Alber, T. (1994) *Nat. Struct. Biol. 1*, 434−438.
29. Creighton, T. E. (1988) *Bioessays 8*, 57−63.
30. Battistoni, A., Mazzetti, A. P., and Rotilio, G. (1999) *FEBS Lett 443*, 313−316.

BI992469G